

Article

Effect of Antioxidants in Medicinal Products on Intestinal Drug Transporters

Chetan P. Kulkarni ^{1,†}, Jia Yang ^{1,†} , Megan L. Koleske ¹, Giovanni Lara ¹, Khondoker Alam ², Andre Raw ³, Bhagwant Rege ³, Liang Zhao ², Dongmei Lu ³, Lei Zhang ², Lawrence X. Yu ³, Robert A. Lionberger ², Kathleen M. Giacomini ¹, Deanna L. Kroetz ^{1,*}  and Sook Wah Yee ^{1,*} 

¹ Department of Bioengineering and Therapeutic Sciences, University of California, San Francisco, CA 94158, USA

² Office of Generic Drugs, Center for Drug Evaluation and Research, FDA, Silver Spring, MD 20993, USA

³ Office of Pharmaceutical Quality, Center for Drug Evaluation and Research, FDA, Silver Spring, MD 20993, USA

* Correspondence: kroetz.3@osu.edu (D.L.K.); sookwah.yee@ucsf.edu (S.W.Y.)

† These authors contributed equally to this work.

Abstract: The presence of mutagenic and carcinogenic N-nitrosamine impurities in medicinal products poses a safety risk. While incorporating antioxidants in formulations is a potential mitigation strategy, concerns arise regarding their interference with drug absorption by inhibiting intestinal drug transporters. Our study screened thirty antioxidants for inhibitory effects on key intestinal transporters—OATP2B1, P-gp, and BCRP in HEK-293 cells (OATP2B1) or membrane vesicles (P-gp, BCRP) using ³H-estrone sulfate, ³H-N-methyl quinidine, and ³H-CCK8 as substrates, respectively. The screen identified that butylated hydroxyanisole (BHA) and carnosic acid inhibited all three transporters (OATP2B1, P-gp, and BCRP), while ascorbyl palmitate (AP) inhibited OATP2B1 by more than 50%. BHA had IC₅₀ values of 71 ± 20 μM, 206 ± 14 μM, and 182 ± 49 μM for OATP2B1, BCRP, and P-gp, respectively. AP exhibited IC₅₀ values of 23 ± 10 μM for OATP2B1. The potency of AP and BHA was tested with valsartan, an OATP2B1 substrate, and revealed IC₅₀ values of 26 ± 17 μM and 19 ± 11 μM, respectively, in HEK-293-OATP2B1 cells. Comparing IC₅₀ values of AP and BHA with estimated intestinal concentrations suggests an unlikely inhibition of intestinal transporters at clinical concentrations of drugs formulated with antioxidants.

Keywords: nitrosamine; antioxidants; intestinal transporters; OATP2B1; BCRP; P-gp



Citation: Kulkarni, C.P.; Yang, J.; Koleske, M.L.; Lara, G.; Alam, K.; Raw, A.; Rege, B.; Zhao, L.; Lu, D.; Zhang, L.; et al. Effect of Antioxidants in Medicinal Products on Intestinal Drug Transporters. *Pharmaceutics* **2024**, *16*, 647. <https://doi.org/10.3390/pharmaceutics16050647>

Academic Editor: Graciela Pavon-Djavid

Received: 1 April 2024

Revised: 2 May 2024

Accepted: 2 May 2024

Published: 10 May 2024



Copyright: © 2024 by the authors. Licensee MDPI, Basel, Switzerland. This article is an open access article distributed under the terms and conditions of the Creative Commons Attribution (CC BY) license (<https://creativecommons.org/licenses/by/4.0/>).

1. Introduction

Since the discovery of N-nitrosamine impurities in valsartan in 2018 [1], multiple batches of other drugs such as metformin, ranitidine, and varenicline have been found to contain these impurities. The International Council for Harmonisation of Technical Requirements for Pharmaceuticals for Human Use (ICH) M7 has classified N-nitrosamines, which are formed by secondary or tertiary amines in the presence of nitrosating agents and contain a functional N-nitroso group (>N-N=O), as possible carcinogens [2,3]. Upon exposure, N-nitrosamines can cause genotoxic effects, which can affect important cellular pathways [4,5]. There have been instances where impurities have arisen from oxidation of the active pharmaceutical ingredient itself, for example, nitroso-varenicline and nitroso-propranolol [6]. In general, N-nitrosamine impurities in medications pose a mutagenic and carcinogenic risk, affecting patient safety [7]. The US Food and Drug Administration (FDA), the European Medicines Agency (EMA), and other regulatory agencies have issued guidance for recommending the control of N-nitrosamine impurities in human drugs [8,9].

There are several measures that were put in place to mitigate N-nitrosamine impurities in pharmaceuticals [10]. N-nitrosamine formation can occur due to nitrite in excipients and vulnerable amines associated with the drug manufacturing process or the active pharmaceutical ingredient itself. Recent studies show that antioxidants such as ascorbic acid, sodium ascorbate, α-tocopherol, caffeic acid, and ferulic acid can effectively inhibit

N-nitrosamine formation in oral solid dosage forms [11–13]. The use of amino acids like glycine, lysine, and histidine as inhibitors in solution has also been suggested [12].

While antioxidants are included in oral medicinal products to enhance drug stability, their potential impact on drug absorption by inhibiting intestinal transporters is unknown [14–16]. Intestinal transporters, which are crucial for the absorption of many prescription drugs, include P-glycoprotein (P-gp, MDR1, ABCB1), breast cancer resistance protein (BCRP, ABCG2), and organic anion transporting polypeptide 2B1 (OATP2B1, SLCO2B1) [17–19]. Numerous clinical studies have shown that inhibition of these transporters can modulate drug bioavailability or exposure. For example, (i) erythromycin, a P-gp inhibitor, increased the bioavailability of the P-gp substrates digoxin and talinolol [20]; (ii) ML753286, a potent BCRP inhibitor, increased exposure to the BCRP substrates sulfasalazine in monkeys [21]; and (iii) grapefruit, apple, and orange juices were reported to reduce exposure to the OATP2B1 drug substrates fexofenadine and aliskiren [22,23]. Our study aimed to understand the potential liabilities of various antioxidants to these intestinal transporters and their impact on drug absorption. A total of 30 antioxidants were screened for their potential to inhibit these transporters. The findings hold significance for generic and new medicinal products, as they are required to demonstrate bioequivalence or comparative bioavailability of the reformulated medicinal product. Introducing an antioxidant into an existing medicinal product constitutes the creation of a new drug formulation. This change generally necessitates a bioequivalence assessment through an *in vivo* clinical bioequivalence study. However, for certain drugs that meet specific criteria, an *in vitro* bridging study may support the reformulation [24]. If sufficient evidence suggests that commonly used antioxidants in oral medicinal products do not significantly affect the activity of the intestinal transporters involved in drug absorption, this could serve as one basis for a waiver of the requirement to provide data from a clinical bioequivalence study for the reformulated products.

2. Materials and Methods

2.1. Oral Antioxidant Library and Reagents

The University of California San Francisco (UCSF)–Stanford CERSI Excipients Browser (<http://excipients.ucsf.bkslab.org/excipients/molecular/?route=oral>, access date: 7 May 2022) and the FDA Inactive Ingredient Database (<https://www.accessdata.fda.gov/scripts/cder/iig/index.cfm>, access date: 7 May 2022) were reviewed to obtain a comprehensive list of 30 antioxidants used in formulations and some known naturally occurring antioxidants. This list was carefully curated by removing duplicates, antioxidants that were no longer in use, those with solubility issues, commercially unavailable ones, and those used in inhalation medicinal products. Additional information on the antioxidants is provided in Table S1. Figure 1 illustrates an overview of the screening process. The initial phase of this study involved identifying antioxidants that demonstrated a significant inhibitory effect ($\geq 50\%$ inhibition) toward the selected transporter function. These antioxidants were then subjected to further analysis through inhibition potency studies (half maximal inhibitory concentration, IC_{50}). We chose to screen the antioxidants at high concentrations, specifically 200 μM , to ensure the detection of any putative transport inhibitors. Positive controls cyclosporin A, verapamil, erlotinib, curcumin, elacridar, and Ko-143, and the transporter substrates digoxin and prazosin, were all purchased from Sigma-Aldrich, (St. Louis, MI, USA); the positive control bromosulfophthalein (BSP) was purchased from Pfaltz & Bauer (Waterbury, CT, USA). ^3H -N-methylquinidine (^3H -NMQ) and ^3H -valsartan were purchased from American Radiolabeled Chemicals (St. Louis, MI, USA), and ^3H -cholecystokinin-8 (^3H -CCK8), ^3H -estrone sulfate (^3H -ES), ^3H -prazosin, and ^3H -digoxin were purchased from PerkinElmer (Waltham, MA, USA). P-gp vesicles (ThermoFisher Scientific, #GM0015; Waltham, MA, USA), BCRP vesicles (ThermoFisher Scientific, #GM0008), Isoplate 96-well flat-bottom white plates (PerkinElmer; # 6005070), filtration plates (Millipore, Burlington, MA, USA), Corning BioCoat poly-D-lysine 48-well plate (#356509, Fisher Scientific), Falcon 24 multiwell inserts (#351181, Corning Life Sciences, Corning, NY, USA), 24-well plate

(#353047, Corning Life Sciences), Hanks' balanced salt solution (HBSS; Gibco, Waltham, MA, USA), bovine serum albumin (BSA; Sigma-Aldrich), Dulbecco's modified Eagle medium (DMEM; Gibco), fetal bovine serum (FBS; Gibco), penicillin and streptomycin (Gibco), glutamine (Gibco), hygromycin B (ThermoFisher Scientific), DMEM with Gluta-Max™ (Gibco), geneticin (Gibco), phosphate-buffered saline (PBS; Gibco), ploy-D-lysine (Gibco), Pierce™ BCA protein assay kit (ThermoFisher Scientific), lucifer yellow (Sigma-Aldrich), EcoLite(+)[™] liquid scintillation cocktail (MP biomedical, Burlingame, CA, USA), and scintillation fluid (MicroScint-20 from PerkinElmer) were purchased from the indicated suppliers.



Figure 1. Overview of the screening process.

2.2. Vesicular Transport Assay

The vesicular transport assay was performed using *Spodoptera frugiperda* 9 (Sf9) membrane vesicles overexpressing human P-gp or BCRP, as reported previously with minor modifications [14,16,25]. In brief, Isoplate 96-well flat-bottom white plates were preincubated with HBSS containing 0.5 mg/mL BSA on an orbital shaker in a 37 °C incubator at 90 rpm for 60 min followed by washing with HBSS. The assay mixture (75 µL/well) contained a probe substrate and either vehicle control, a known inhibitor of P-gp or BCRP, or an antioxidant, in vesicle uptake buffer (50 mM MOPS-Tris, pH 7.0 + 70 mM KCl + 7.5 mM MgCl₂) prewarmed to 37 °C. After addition of the assay mixture, 5 µL/well (5 µg/µL stock concentration of the vesicles) of vesicles overexpressing human P-gp or BCRP was added. Uptake assays were initiated by adding 20 µL of either 25 mM adenosine triphosphate (ATP) or 25 mM adenosine monophosphate (AMP) to a final concentration of 5 mM. Plates were incubated at 37 °C for 20 min with orbital shaking (90 rpm). After 20 min, the uptake was quenched by adding 150 µL of ice-cold wash buffer (40 mM MOPS-Tris, pH 7.0 + 70 mM KCl) to each well, and the mixture was transferred to a 96-well filtration plate. Vacuum was applied, and the vesicles were washed three times with wash buffer. Vesicles were then lysed with 100 µL of MicroScint-20. The 96-well plates were placed on a shaker at room temperature for 1–2 h prior to measuring the radioactivity by liquid scintillation counting with a MicroBeta²[®] microplate counter.

2.3. Cell Lines and Cell Culture

Human embryonic kidney (HEK) 293 cells overexpressing OATP2B1 (HEK-293-OATP2B1) were cultured and maintained in DMEM supplemented with 10% fetal bovine serum, penicillin (100 U/mL), streptomycin (100 µg/mL), 2 mM glutamine, and 100 µg/mL of hygromycin B at 37 °C in a humidified incubator with 5% CO₂. MDCK-hMDR1-cMDR1-KO cells, with the endogenous canine MDR1 gene knockout and stable expression of human MDR1, and MDCK-hBCRP-cMDR1-KO cells, with the endogenous canine MDR1 gene knockout and stable expression of human BCRP, were generously provided by Dr. Per Artursson from Uppsala University, along with the corresponding MDCK-cMDR1-KO cells [14,26–28]. Cells were cultured in T-25 flasks in DMEM with Gluta-Max™, supplemented with 10% fetal bovine serum, penicillin (100 U/mL), and streptomycin (100 µg/mL). For MDCK cells overexpressing hMDR1, the media were further supplemented with hygromycin B (400 µg/mL), and, for MDCK cells overexpressing hBCRP, the media were supplemented with geneticin

(600 µg/mL). The cells were maintained at 37 °C in a humidified incubator with 5% CO₂. Cells were only utilized through passage 4.

2.4. Uptake Transporter Assay

The uptake transporter assay was performed as reported previously with minor modifications [15]. A day before the uptake assay, Isoplate 96-well plates were coated with poly-D-lysine in PBS with calcium and magnesium and washed with PBS. HEK-293-OATP2B1 cells were seeded at a density of 60,000 cells/well. An assay mixture of ³H-estrone sulfate, a known inhibitor of OATP2B1, or an antioxidant was prepared and incubated in a 37 °C incubator for 10 min. The cells were washed with ice-cold HBSS three times and incubated with MicroScint fluid on a shaker for 1 h for cell lysis. Radioactivity was measured by liquid scintillation counting with a MicroBeta²® microplate counter. Similar methods were used to assess the inhibition of ³H-valsartan-mediated uptake by OATP2B1 using the two antioxidants, AP and BHA. One day before the uptake assay, HEK-293-OATP2B1 cells were seeded in a 48-well poly-d-lysine-coated plate at a density of 120,000 cells/well. On the day of experiment, cells were washed twice with 0.4 mL of HBSS per well and then pre-incubated for 10–20 min in 0.4 mL of HBSS. To assess inhibition, the cells were incubated with uptake buffer (trace amount of ³H-valsartan in HBSS) containing either 1% DMSO as negative control, 100 µM erlotinib as positive control, or various concentrations of the antioxidants, AP or BHA. Uptake of ³H-valsartan was stopped after 15 min by washing three times with ice-cold HBSS. Cells were lysed in 750 µL of lysis buffer (0.1 N NaOH and 0.1% SDS in double-distilled water) per well while shaking for 60 min. A total of 690 µL of the lysate from each well was then added to 2.5 mL of EcoLite scintillation fluid. The radioactivity was determined on a LS6500 Scintillation Counter (Beckman Coulter). Protein concentration was measured with a Pierce™ BCA protein assay kit. The radioactivity in each well was corrected for protein concentration. All values were determined in triplicate, and the final values are expressed as % uptake relative to negative control (1% DMSO).

2.5. Antioxidant Screening and IC₅₀ Determination

Antioxidants were screened at a concentration of 200 µM. Screening was carried out in triplicate, and antioxidants that inhibited any of the three transporters by at least 50% were further studied. IC₅₀ estimates of the putative inhibitors were obtained by fitting dose–response data (500 µM to 0.03 µM for OATP2B1 and 500 µM to 4 µM for P-gp and BCRP) to the Hill equation by nonlinear regression in GraphPad Prism 9.

2.6. Estimation of Intestinal Luminal Concentration (*I*_{gut}) Concentration

*I*_{gut} is intestinal luminal concentration estimated as dose/250 mL. The *I*_{gut} concentration was estimated using the following equation:

$$I_{gut} = [A \div (MW \times V)] \times 10^6$$

where *I*_{gut} is the estimated intestinal luminal concentration (µM), *A* is the amount of antioxidant in an oral dosage (mg), *MW* is the molecular weight, and *V* is the volume of intestinal fluid, i.e., 250 mL.

2.7. Transwell Transport Assay

The transport assay was performed using MDCK-hMDR1-cMDR1-KO, MDCK-cMDR1-KO, and MDCK-hBCRP-cMDR1-KO as reported previously with minor modifications [14,27]. In brief, 133,000 cells were seeded onto a Transwell membrane insert, a semipermeable polyethylene terephthalate membrane. During the differentiation process, the medium volume in the apical chamber was kept at 300 µL, while the basal chamber contained 1000 µL. The cells were allowed to differentiate for 7–9 days at 37 °C in a humidified incubator with 5% CO₂. Before starting transporter assays, the integrity of the cell monolayer was checked using lucifer yellow permeability assays. Cells were washed twice with HBSS, lucifer yellow

(0.1 mg/mL) in HBSS was added to the apical chamber, and the basal chamber was filled with fresh HBSS. The assembled plate was then incubated at 37 °C for 1 h. From the basal chamber, 100 µL samples were collected for fluorescence measurements using GloMax® Explorer with a 475 nm excitation filter and a 500–550 nm emission filter to calculate the percent permeability per well.

To assess the flux of digoxin or prazosin from the basal to apical side, the cells were washed twice with HBSS. In the basal chamber, an HBSS solution containing either digoxin (6.35 nM ³H-labeled, final concentration 2.5 µM) or prazosin (43 nM ³H-labeled, final concentration 1 µM) was added either with vehicle or a known or putative inhibitor (elacridar at 2 µM for P-gp, Ko143 at 1 µM for BCRP, or BHA at 250, 178, and 62.5 µM). Simultaneously, the same concentration of these inhibitors in HBSS (225 µL) was added to the apical chamber. The plates were incubated at 37 °C with shaking at 200 rpm. Aliquots of 25 µL were collected from the apical compartment at 0, 1, 2, and 4 h, with corresponding replenishment of the apical solution. Samples (25 µL) were also taken from the basal chambers at the start and at the end of each experiment. These samples were used to calculate the disintegrations per minute/picomole ratio. All apical and basal samples were mixed with scintillation fluid (EcoLite(+)TM liquid scintillation cocktail), and their radioactivity was measured using liquid scintillation counting (Beckman LS6500). At the end of the transport assay, a lucifer yellow permeability assay was performed as described earlier. For data analysis, the disintegration per minute counts of digoxin or prazosin from the apical samples were converted to picomoles using radioactivity measured in the substrate solution.

3. Results

3.1. *In Vitro* Studies Performed to Assess the Inhibition of 30 Antioxidants on OATP2B1, BCRP, and P-gp

In this study, the probe substrates ³H-ES, ³H-CCK8, and ³H-NMQ were used to measure the activities of OATP2B1, BCRP, and P-gp transporters, respectively [15,16,25,29]. As shown in Figure 2, the uptake of the radioactive probe substrate in human BCRP or P-gp membrane vesicles was significantly higher in the presence of ATP compared to AMP: 9.8 times higher for BCRP and 3.9 times higher for P-gp. In addition, the known inhibitors, BSP (for BCRP), and verapamil (for P-gp) significantly reduced the uptake of these probe substrates, confirming the reliability of our assay in measuring transporter-mediated uptake in membrane vesicles. Notably, ³H-NMQ exhibited significant adsorption on the filtration plate (Figure S1), unlike other radioactive probe substrates. In further experiments, as shown in Figure 2, the uptake of ³H-ES in HEK-293 cells expressing OATP2B1 was 37.6 times greater than in cells expressing the empty vector (EV). This uptake was significantly inhibited by erlotinib, a known OATP2B1 inhibitor, indicating the suitability of this model substrate for assessing OATP2B1-mediated transport. The scintillation fluid (MicroScint-20) used in this screening assay was not compatible with BCA protein reagents, so we were unable to normalize each well individually by protein concentration. To assess the variance in protein concentration per well, we conducted radioligand uptake using another plate with identical wash steps and found consistent protein concentrations across wells (Figure S2).

We observed an inhibition of at least 50% for all three transporters with butylated hydroxyanisole (BHA) and carnosic acid. In addition, ascorbyl palmitate (AP) inhibited OATP2B1, and lysine inhibited P-gp. Table 1 summarizes the effect of each of the antioxidants on the activity of the transporters. IC₅₀ values for BHA were 71 ± 20 µM (OATP2B1), 206 ± 14 µM (BCRP), and 182 ± 49 µM (P-gp), and AP inhibited OATP2B1 with an IC₅₀ value of 23 ± 10 µM. Pre-incubation of the OATP2B1-expressing cells with BHA and AP for 30 min did not further affect their inhibition potency (Table S2). Representative IC₅₀ curves for each transporter are presented in Figure 3.

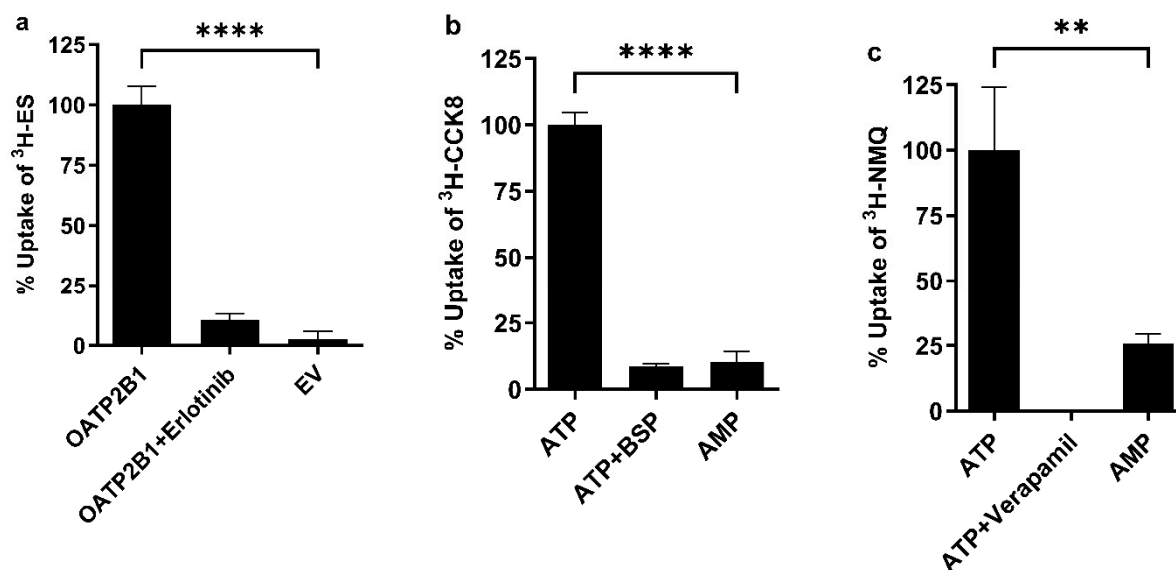


Figure 2. Validation of OATP2B1, BCRP, and P-gp transporter assays. (a) Uptake of ³H-ES by human OATP2B1: HEK-293 cells expressing OATP2B1 ($n = 6$), OATP2B1 in the presence of 20 μ M erlotinib (an OATP2B1 inhibitor; $n = 3$), or an empty vector ($n = 12$) were incubated with ³H-ES at 37 $^{\circ}$ C for 10 min. (b) Uptake of ³H-CCK8 by human BCRP: BCRP membrane vesicles (25 μ g/well) were incubated with ³H-CCK8 with either 5 mM ATP ($n = 6$), 5 mM ATP with 200 μ M BSP ($n = 3$), or 5 mM AMP ($n = 3$) at 37 $^{\circ}$ C for 20 min. (c) Uptake of ³H-NMQ by human P-gp: P-gp membrane vesicles (25 μ g/well) were incubated with ³H-NMQ in the presence of 5 mM ATP ($n = 6$), 5 mM ATP with 200 μ M verapamil ($n = 3$), or 5 mM AMP ($n = 3$) at 37 $^{\circ}$ C for 20 min. Transport in the absence of inhibitors is expressed as 100% and each value represents the mean \pm SD; a two-tailed t -test was applied $p < 0.0001$: ****; $p < 0.01$: **.

Table 1. Inhibition of transporter activity by antioxidants. The uptake of a probe substrate was measured in the presence of an antioxidant (200 μ M) or DMSO. The uptake from cells treated with DMSO was set as 100% and the uptake with the indicated antioxidants is presented as a percentage of this reference level. The values reported are the mean \pm standard deviation (SD) from three replicates. Only ascorbyl palmitate (AP), butylated hydroxyanisole (BHA), carnosic acid, and lysine met the predetermined threshold for putative inhibitors of 50% inhibition. AP and BHA were selected for further evaluation because they are commonly utilized in oral drug formulations and are also included in the FDA's Inactive Ingredients Database (IID).

Compounds	% Uptake of ³ H-ES	% Uptake of ³ H-CCK8	% Uptake of ³ H-NMQ
	OATP2B1	BCRP	P-gp
Ascorbic acid	103.6 \pm 9.3	92.7 \pm 5.9	113.6 \pm 43.3
Ascorbyl palmitate (AP)	28.3 \pm 11.2	50.9 \pm 9.9	86.9 \pm 12.4
Butylated hydroxytoluene (BH)	137.1 \pm 34.8	102.8 \pm 9.2	98.1 \pm 20.3
Cysteine hydrochloride	106.5 \pm 14.8	90.0 \pm 12.5	134.8 \pm 41.1
Propyl gallate	79.3 \pm 17.2	86.5 \pm 2.6	149.1 \pm 67.6
Vitamin E	83.5 \pm 20.9	81.0 \pm 12.6	67.9 \pm 24
3,4-dihydroxybenzoid acid	85.4 \pm 4.4	78.5 \pm 6.9	118.9 \pm 20

Table 1. Cont.

Compounds	% Uptake of ³ H-ES	% Uptake of ³ H-CCK8	% Uptake of ³ H-NMQ
	OATP2B1	BCRP	P-gp
Anhydrous citric acid	128.8 ± 24.4	93.1 ± 6.7	92 ± 2.1
Butylated hydroxyanisole (BHA)	19.8 ± 7.1	46.7 ± 5.5	42.1 ± 5.7
Caffeic acid	119.8 ± 19.8	75.8 ± 3.7	133.8 ± 12
Carnosic acid	18.8 ± 5.6	4.5 ± 4.8	0.0 ± 10.1
Carnosine	119.3 ± 27.6	99.7 ± 11.6	82.6 ± 44
Co-enzyme Q-10	116.1 ± 16.0	82.7 ± 16.2	90.3 ± 16.3
EDTA (edetate disodium)	112.8 ± 25.2	110.4 ± 24.6	69.3 ± 20.5
Ergothioneine	118.2 ± 30.6	112.5 ± 11.2	58.2 ± 23.6
Erythorbic acid	123.3 ± 15.0	88.2 ± 7.5	81.8 ± 31.4
Ferulic acid	136.4 ± 20.7	91.0 ± 4.7	100.4 ± 16.6
Glutathione	107.9 ± 7.8	95.9 ± 2.2	79.8 ± 15.8
Glycine	125.6 ± 23.0	99.7 ± 15.1	76.9 ± 4.1
Histidine	108.9 ± 4.0	92.4 ± 1.6	87.6 ± 10.6
Lysine	120.3 ± 21.4	109.0 ± 20.8	32.5 ± 44.3
Methionine	113.2 ± 15.2	94.8 ± 9.4	86.7 ± 24.5
Phosphoric acid	97.8 ± 5.0	83.0 ± 18.0	83.1 ± 27.6
Potassium sorbate	98.8 ± 19.8	104.8 ± 14.5	103.5 ± 28.7
Sesamol	103.1 ± 7.2	90.3 ± 3.7	121.3 ± 35.1
Sodium bisulfite	90.1 ± 24.5	110.4 ± 9.3	96.1 ± 30.4
Sodium metabisulfite	118.9 ± 31.7	94.5 ± 8.2	78.8 ± 17.5
Sodium sulfite	92.9 ± 4.5	99.7 ± 5.5	77.7 ± 33.7
Sodium thiosulfate, pentahydrate	104.4 ± 2.4	114.2 ± 22.8	77.4 ± 20
Tartaric acid	101.1 ± 5.8	96.9 ± 16.6	108 ± 10.8
Cyclosporin A	83.3 ± 18.6	8.3 ± 4.5	0.0 ± 10.3
Verapamil	194.2 ± 36.4	50.5 ± 6.8	0.0 ± 6
Bromosulfophthalein	10.9 ± 8.1	0.3 ± 1.2	0.0 ± 22
Erlotinib	10.5 ± 2.8	58.5 ± 3.9	63 ± 5
Curcumin	8.2 ± 2.4	0.0 ± 1.8	0.0 ± 2.8

Positive Control

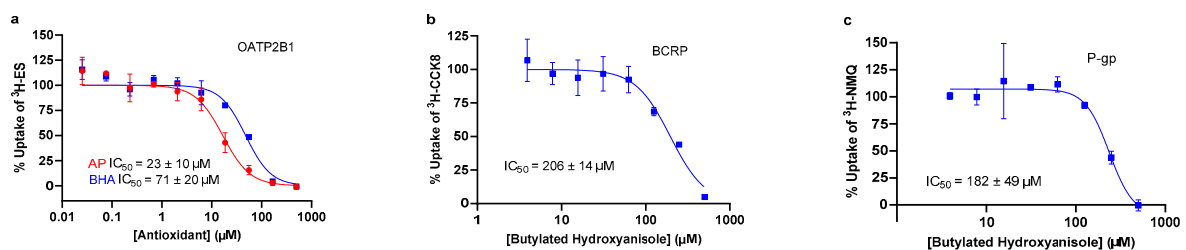


Figure 3. Concentration–response relationships for inhibition of intestinal transporters by AP and BHA. (a) AP and BHA inhibition of OATP2B1; (b) BHA inhibition of BCRP; (c) BHA inhibition of P-gp. Reported IC₅₀s are the mean ± SD of three independent experiments. Plots show the mean ± SD from one representative experiment.

3.2. Comparison of AP and BHA IC_{50} Values with the Estimated Intestinal Concentrations

We compared the IC_{50} values of AP and BHA with their estimated intestinal concentrations to determine whether they may potentially interfere clinically with the transporters to affect oral bioavailability. As shown in Table 2, the I_{gut}/IC_{50} ratios were less than 10 for both AP and BHA [30]. If I_{gut}/IC_{50} was less than 10, the potential of the inhibitor to inhibit the transporter in vivo was considered low [31].

Table 2. Comparison of IC_{50} values of the antioxidants with estimated intestinal concentrations. (a). Estimated maximum concentrations of AP and BHA in intestinal fluid. (b). The ratio between the estimated intestinal concentration (I_{gut}) of AP and BHA and the inhibition potencies (IC_{50}) of the respective transporters. ND—not determined, as AP does not inhibit P-gp and BCRP by $\geq 50\%$ at a concentration of 200 μM .

(a)				
Compound	MW (g/mol)	FDA IID Oral Limit (mg/day)	% <i>w/w</i> in 500 mg Oral Unit	Max Intestinal Conc (μM) in 250 mL Fluid
Ascorbyl palmitate (AP)	414.53	12	2% (10 mg)	96.5
Butylated hydroxyanisole (BHA)	180.24	8	1.6% (8 mg)	178
(b)				
Transporter	I_{gut}/IC_{50}			
	AP	BHA		
OATP2B1	4.2	2.5		
BCRP	ND	0.9		
P-gp	ND	1.0		

3.3. Effect of AP and BHA on OATP2B1-Mediated Valsartan Uptake

Numerous essential medicinal products faced recalls from the market due to the presence of N-nitrosamine impurities [10,32], and some of these medicinal products are substrates of the transporters that we investigated. A potential strategy used to address this issue involves incorporating antioxidants into the products to prevent N-nitrosamine formation due to degradation. We aimed to examine the effect of antioxidants on the transport of a drug substrate that had been subject to recalls due to the presence of N-nitrosamine impurities in certain lots [10]. Valsartan, a drug recognized as a substrate of OATPs [33], was chosen for this investigation. The average IC_{50} values for OATP2B1, derived from three independent experiments, were $25.5 \pm 16.8 \mu M$ for AP and $19.1 \pm 11.1 \mu M$ for BHA. Figure 4 represents data from one experiment. The calculated I_{gut}/IC_{50} ratios for AP and BHA were 3.8 and 9.3, respectively, both below the threshold of 10 [30].

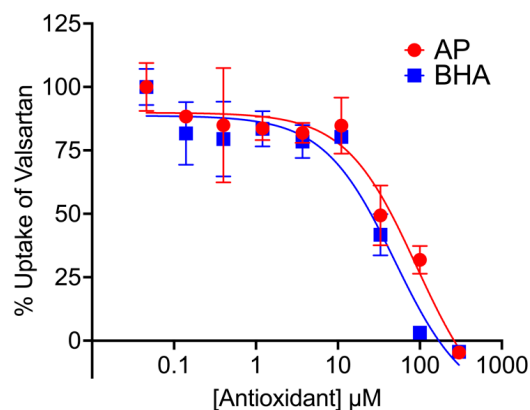


Figure 4. Concentration–response relationships for inhibition of OATP2B1-mediated valsartan transport by AP and BHA. Plots show mean \pm SD from one representative experiment.

3.4. Effects of Elacridar or BHA on the Transport of Digoxin Efflux in Transwell Assays

We evaluated the effect of BHA on inhibiting digoxin transport by P-gp using a transwell assay. The basal-to-apical flux of digoxin was approximately three- to five-fold higher in MDCK cells overexpressing human MDR1 compared to control cells that do not express canine or human MDR1. Treatment with elacridar (2 μ M), a known P-gp inhibitor, diminished digoxin transport in the human MDR1-overexpressing cells to levels similar to those in the control cells, indicating the specific transport of digoxin by P-gp (Figure 5). The calculated maximal intestinal concentration of BHA (178 μ M), assuming the ingestion of the maximum BHA dose (8 mg) from an oral formulation in 250 mL of intestinal fluid, was tested for its capability to inhibit P-gp. Neither the estimated maximal intestinal concentration of 178 μ M nor a lower concentration (62.5 μ M) inhibited digoxin transport (Figure 5). Notably, a higher concentration of BHA (250 μ M) disrupted MDCK cell tight junctions as indicated by increased lucifer yellow permeability, precluding further assays to estimate P-gp inhibition by BHA.

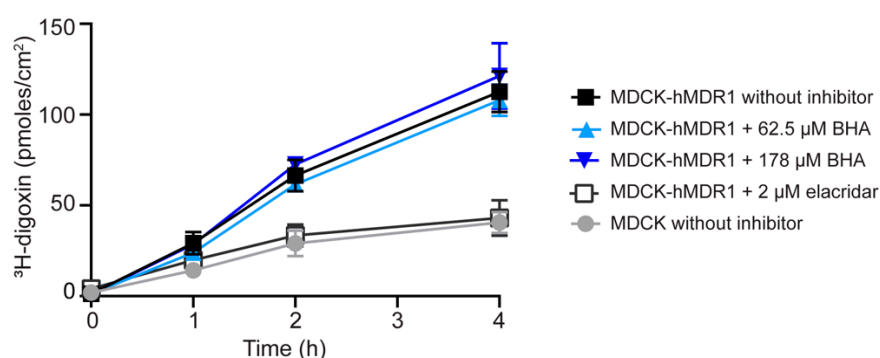


Figure 5. Effects of elacridar or BHA on the efflux of digoxin by MDCK-hMDR1-cMDR1-KO cells. The MDCK-hMDR1-cMDR1-KO cell line is a CRISPR-Cas9 engineered MDCK line that expresses human MDR1 while lacking the endogenous canine MDR1 (cABCB1). Elacridar (2 μ M) or BHA (62.5 or 178 μ M) was applied to both the basal and apical sides of the cells. The control cell line was MDCK, in which the canine MDR1 (cABCB1) has been knocked out. The efflux of ³H-digoxin (2.5 μ M) from the basal to apical side was measured over a period of 4 h, both with and without the addition of the compounds to both sides. Data are presented as mean values \pm SD from one representative experiment.

4. Discussion

Antioxidants have potential as nitrite scavengers to mitigate N-nitrosamine formation in medicinal products [12,34]. In this study, we characterized the interactions of antioxidants used in oral formulations with three major intestinal transporters (OATP2B1, P-gp, and BCRP). Antioxidants are often added to oral pharmaceuticals to improve drug stability, but their potential impact on drug absorption by inhibiting these major intestinal drug transporters has not been extensively tested. Inhibition of these transporters can significantly alter drug bioavailability, as evidenced in clinical studies [20–23]. In the current work, we screened a panel of 30 molecular excipients with antioxidant properties to assess their ability to modulate the function of OATP2B1 using HEK-293 cells expressing this transporter. Additionally, we examined the effects of these excipients on BCRP and P-gp using membrane vesicles expressing each transporter. Carnosic acid and BHA emerged as significant inhibitors ($\geq 50\%$ inhibition) of the uptake of canonical substrates by all three transporters at a concentration of 200 μ M. AP and lysine showed inhibitory activity only against OATP2B1 and P-gp, respectively. Although carnosic acid has been identified as a P-gp inhibitor in ATPase assays [35], carnosic acid was excluded from further consideration as the compound is not an FDA-approved inactive ingredient. Lysine was also not selected for further study, as lysine is a common ingredient in FDA-approved injectables rather than in oral dose formulations (<https://www.accessdata.fda.gov/scripts/cder/iig/index.cfm>,

access date: 31 August 2022). To the best of our knowledge, this study was the first to evaluate the majority of these antioxidant excipients for their potential impact on major intestinal transporters. This study includes four antioxidants (i.e., (\pm) - α -tocopherol, butylated hydroxytoluene, L-ascorbic acid, and sodium thiosulfate) that were previously assessed and found not to inhibit these transporters [14–16]. Our findings provide data for the informed selection and evaluation of antioxidants in oral dosage forms.

To further evaluate the potential clinical relevance of BHA and AP, two antioxidants that interact with the three major intestinal transporters OATP2B1, BCRP, and P-gp, we estimated their maximal intestinal concentrations based on the maximum allowable oral amount set by the World Health Organization and the Code of Federal Regulations Title 21. According to the FDA's guidance on the role of transporters in drug–drug interactions affecting intestinal absorption [30], excipients with $I_{\text{gut}}/IC_{50} \geq 10$ (I_{gut} , estimated maximal intestinal concentration) could potentially inhibit transporter-mediated drug absorption in clinical settings [30,31,36]. As shown in Table 2, the I_{gut}/IC_{50} values for both BHA and AP are significantly lower than 10, suggesting minimal potential for the inhibition of OATP2B1, BCRP, and P-gp at the maximum expected concentration in the intestinal lumen. Furthermore, the I_{gut}/IC_{50} ratios for BHA and AP, using valsartan as the drug substrate, were below the threshold of 10. Hence, it is unlikely that AP and BHA would significantly inhibit the OATP2B1-mediated uptake of valsartan clinically.

A crucial question remains as to whether the inhibition observed in inside-out vesicle assays for BCRP and P-gp translates to in vivo settings. To replicate the in vivo environment, we performed cellular efflux assays using BCRP- and P-gp-overexpressing MDCK cells, introducing the antioxidant into the culture medium. Notably, elacridar, a canonical P-gp inhibitor, effectively blocked digoxin efflux in our P-gp-overexpressing cell system, validating the suitability of a whole-cell system for P-gp inhibitor screening (Figure 5). In contrast to the vesicular assay, BHA did not impede digoxin transport in MDCK cells overexpressing P-gp, even at the maximal intestinal concentration of 178 μM . Additionally, we evaluated BHA's interaction with BCRP using prazosin, a prototypical BCRP substrate, in MDCK cells. Similarly, 178 μM of BHA did not inhibit prazosin efflux in MDCK cells overexpressing BCRP, while Ko143, a BCRP inhibitor, significantly reduced prazosin transport (Figure S3).

The observed discrepancies between the results of the vesicular and cellular efflux assays could stem from several factors. First, cells, unlike single vesicles, are complex and integrated with a multitude of receptors, metabolic enzymes, and transporters. This intricate environment may hinder the effective penetration of BHA to the vicinity of intracellular BCRP and P-gp, potentially preventing the accumulation of sufficient concentrations to inhibit their transport activity. Furthermore, the substrates employed in the vesicular and cellular assays differ, potentially exhibiting distinct transport mechanisms. These structural variations among the substrates could influence their interactions with specific residues within the corresponding transporters, thereby affecting inhibitory potential. Therefore, caution should be exercised when extrapolating results from inside-out membrane vesicles to whole cells or in vivo situations.

In conclusion, the antioxidant BHA was identified as an inhibitor of the intestinal drug transporters OATP2B1, BCRP, and P-gp. However, when comparing the IC_{50} values and the intestinal concentration of the antioxidant in the intestinal fluid, it suggests that the potential of BHA to inhibit the transporter in vivo was considered low for these transporters. Our findings provide data on the potential impact of antioxidants on the intestinal absorption and efflux of various drugs. Our results indicate that many antioxidants do not interact with OATP2B1, BCRP, and P-gp in cells, making them suitable candidates for use in oral dosage forms to inhibit the formation of N-nitrosamine impurities without compromising the bioavailability of co-administered drugs.

Supplementary Materials: The following supporting information can be downloaded at: <https://www.mdpi.com/article/10.3390/pharmaceutics16050647/s1>, Figure S1: 3H-NMQ adsorbs on the filtration plate; Figure S2: Protein concentration per well was consistent; Figure S3: Effects of Ko 143 or BHA on the efflux of Prazosin by MDCK-hBCRP-cMDR1-KO cells; Table S1: Antioxidant screened for P-gp, BCRP and OATP2B1-mediated uptake inhibition; Table S2: Comparison of IC₅₀ values obtained with and without preincubation of the OATP2B1 expressing cells with BHA and AP.

Author Contributions: Conceptualization, S.W.Y., D.L.K. and K.M.G.; methodology, S.W.Y., D.L.K., C.P.K., J.Y., M.L.K. and G.L.; validation, C.P.K., J.Y. and M.L.K.; formal analysis, C.P.K., J.Y. and M.L.K.; investigation, C.P.K., J.Y. and M.L.K.; resources, S.W.Y., D.L.K. and K.M.G.; data curation, G.L.; writing—original draft preparation, S.W.Y., C.P.K., J.Y. and G.L.; writing—review and editing, S.W.Y., C.P.K., J.Y., K.A., A.R., B.R., L.Z. (Liang Zhao), D.L., L.Z. (Lei Zhang), L.X.Y., R.A.L., K.M.G., S.W.Y. and D.L.K.; visualization, C.P.K., J.Y., M.L.K. and G.L.; supervision, S.W.Y. and D.L.K.; project administration, S.W.Y., D.L.K., K.A., A.R., B.R., L.Z. (Liang Zhao), L.X.Y., R.A.L., D.L. and L.Z. (Lei Zhang); funding acquisition, S.W.Y., D.L.K., K.M.G., K.A., A.R., B.R., L.Z. (Liang Zhao), D.L., L.X.Y., R.A.L. and L.Z. (Lei Zhang) All authors have read and agreed to the published version of the manuscript.

Funding: This research was funded by U.S. Food and Drug Administration Grant U01FD005978, which supports the University of California, San Francisco–Stanford Center of Excellence in Regulatory Sciences and Innovation (UCSF–Stanford CERSI).

Institutional Review Board Statement: Not applicable.

Informed Consent Statement: Not applicable.

Data Availability Statement: The original contributions presented in the study are included in the article/Supplementary Materials, further inquiries can be directed to the corresponding author.

Acknowledgments: We wish to thank Per Artursson and Maria Karlgren from Uppsala University for providing MDCK-hMDR1-cMDR1-KO, MDCK-hBCRP-cMDR1-KO, and MDCK-cMDR1-KO cells. We would also like to express our gratitude to Ruchika Bajaj for her insights regarding Transwell assays.

Conflicts of Interest: The authors declare no conflict of interest. Disclaimer: The views expressed here do not reflect the official policies of the U.S. FDA or the Department of Health and Human Services, nor does any mention of trade names imply endorsement by the U.S. Government.

References

1. Information about Nitrosamine Impurities in Medications. Available online: <https://www.fda.gov/drugs/drug-safety-and-availability/information-about-nitrosamine-impurities-medications> (accessed on 20 December 2023).
2. Dobo, K.L.; Kenyon, M.O.; Dirat, O.; Engel, M.; Fleetwood, A.; Martin, M.; Mattano, S.; Musso, A.; McWilliams, J.C.; Papanikolaou, A.; et al. Practical and Science-Based Strategy for Establishing Acceptable Intakes for Drug Product N-Nitrosamine Impurities. *Chem. Res. Toxicol.* **2022**, *35*, 475–489. [CrossRef] [PubMed]
3. Paglialunga, S.; van Haarst, A. The Impact of N-Nitrosamine Impurities on Clinical Drug Development. *J. Pharm. Sci.* **2023**, *112*, 1183–1191. [CrossRef] [PubMed]
4. Johnson, G.E.; Dobo, K.; Gollapudi, B.; Harvey, J.; Kenny, J.; Kenyon, M.; Lynch, A.; Minocherhomji, S.; Nicolette, J.; Thybaud, V.; et al. Permitted Daily Exposure Limits for Noteworthy N-Nitrosamines. *Environ. Mol. Mutagen.* **2021**, *62*, 293–305. [CrossRef] [PubMed]
5. Li, Y.; Hecht, S.S. Metabolic Activation and DNA Interactions of Carcinogenic N-Nitrosamines to Which Humans Are Commonly Exposed. *Int. J. Mol. Sci.* **2022**, *23*, 4559. [CrossRef] [PubMed]
6. Schlingemann, J.; Burns, M.J.; Ponting, D.J.; Martins Avila, C.; Romero, N.E.; Jaywant, M.A.; Smith, G.F.; Ashworth, I.W.; Simon, S.; Saal, C.; et al. The Landscape of Potential Small and Drug Substance Related Nitrosamines in Pharmaceuticals. *J. Pharm. Sci.* **2023**, *112*, 1287–1304. [CrossRef] [PubMed]
7. Moser, J.; Ashworth, I.W.; Harris, L.; Hillier, M.C.; Nanda, K.K.; Scrivens, G. N-Nitrosamine Formation in Pharmaceutical Solid Drug Products: Experimental Observations. *J. Pharm. Sci.* **2023**, *112*, 1255–1267. [CrossRef] [PubMed]
8. Control of Nitrosamine Impurities in Human Drugs. Available online: <https://www.fda.gov/regulatory-information/search-fda-guidance-documents/control-nitrosamine-impurities-human-drugs> (accessed on 20 December 2023).
9. Nitrosamine Impurities. Available online: <https://www.ema.europa.eu/en/human-regulatory-overview/post-authorisation/pharmacovigilance-post-authorisation/referral-procedures-human-medicines/nitrosamine-impurities> (accessed on 20 December 2023).
10. Tuesuwan, B.; Vongsutitlers, V. Nitrosamine Contamination in Pharmaceuticals: Threat, Impact, and Control. *J. Pharm. Sci.* **2021**, *110*, 3118–3128. [CrossRef]

11. Shakleya, D.; Asmelash, B.; Alayoubi, A.; Abrigo, N.; Mohammad, A.; Wang, J.; Zhang, J.; Yang, J.; Marzan, T.A.; Li, D.; et al. Bumetanide as a Model NDSRI Substrate: N-Nitrosobumetanide Impurity Formation and Its Inhibition in Bumetanide Tablets. *J. Pharm. Sci.* **2023**, *112*, 3075–3087. [[CrossRef](#)] [[PubMed](#)]
12. Nanda, K.K.; Tignor, S.; Clancy, J.; Marota, M.J.; Allain, L.R.; D’Addio, S.M. Inhibition of N-Nitrosamine Formation in Drug Products: A Model Study. *J. Pharm. Sci.* **2021**, *110*, 3773–3775. [[CrossRef](#)]
13. Bayne, A.-C.V.; Mistic, Z.; Stemmler, R.T.; Wittner, M.; Frerichs, M.; Bird, J.K.; Besheer, A. N-Nitrosamine Mitigation with Nitrite Scavengers in Oral Pharmaceutical Drug Products. *J. Pharm. Sci.* **2023**, *112*, 1794–1800. [[CrossRef](#)]
14. Bajaj, R.; Chong, L.B.; Zou, L.; Tsakalozou, E.; Ni, Z.; Giacomini, K.M.; Kroetz, D.L. Interaction of Commonly Used Oral Molecular Excipients with P-Glycoprotein. *AAPS J.* **2021**, *23*, 106. [[CrossRef](#)] [[PubMed](#)]
15. Zou, L.; Spanogiannopoulos, P.; Pieper, L.M.; Chien, H.-C.; Cai, W.; Khuri, N.; Pottel, J.; Vora, B.; Ni, Z.; Tsakalozou, E.; et al. Bacterial Metabolism Rescues the Inhibition of Intestinal Drug Absorption by Food and Drug Additives. *Proc. Natl. Acad. Sci. USA* **2020**, *117*, 16009–16018. [[CrossRef](#)] [[PubMed](#)]
16. Zou, L.; Pottel, J.; Khuri, N.; Ngo, H.X.; Ni, Z.; Tsakalozou, E.; Warren, M.S.; Huang, Y.; Shoichet, B.K.; Giacomini, K.M. Interactions of Oral Molecular Excipients with Breast Cancer Resistance Protein, BCRP. *Mol. Pharm.* **2020**, *17*, 748–756. [[CrossRef](#)]
17. Iversen, D.B.; Andersen, N.E.; Dalgård Dunvald, A.-C.; Pottegård, A.; Stage, T.B. Drug Metabolism and Drug Transport of the 100 Most Prescribed Oral Drugs. *Basic. Clin. Pharmacol. Toxicol.* **2022**, *131*, 311–324. [[CrossRef](#)] [[PubMed](#)]
18. Brackman, D.J.; Giacomini, K.M. Reverse Translational Research of ABCG2 (BCRP) in Human Disease and Drug Response. *Clin. Pharmacol. Ther.* **2018**, *103*, 233–242. [[CrossRef](#)] [[PubMed](#)]
19. McFeely, S.J.; Wu, L.; Ritchie, T.K.; Unadkat, J. Organic Anion Transporting Polypeptide 2B1- More than a Glass-Full of Drug Interactions. *Pharmacol. Ther.* **2019**, *196*, 204–215. [[CrossRef](#)] [[PubMed](#)]
20. Schwarz, U.I.; Gramatté, T.; Krappweis, J.; Oertel, R.; Kirch, W. P-Glycoprotein Inhibitor Erythromycin Increases Oral Bioavailability of Talinolol in Humans. *Int. J. Clin. Pharmacol. Ther.* **2000**, *38*, 161–167. [[CrossRef](#)]
21. Zhang, Y.; Shipkova, P.A.; Warrack, B.M.; Nelson, D.M.; Wang, L.; Huo, R.; Chen, J.; Panfen, E.; Chen, X.-Q.; Fancher, R.M.; et al. Metabolomic Profiling and Drug Interaction Characterization Reveal Riboflavin as a Breast Cancer Resistance Protein-Specific Endogenous Biomarker That Demonstrates Prediction of Transporter Activity in Vivo. *Drug Metab. Dispos.* **2023**, *51*, 851–861. [[CrossRef](#)] [[PubMed](#)]
22. Dresser, G.K.; Bailey, D.G.; Leake, B.F.; Schwarz, U.I.; Dawson, P.A.; Freeman, D.J.; Kim, R.B. Fruit Juices Inhibit Organic Anion Transporting Polypeptide-Mediated Drug Uptake to Decrease the Oral Availability of Fexofenadine. *Clin. Pharmacol. Ther.* **2002**, *71*, 11–20. [[CrossRef](#)]
23. Chen, M.; Zhou, S.-Y.; Fabriaga, E.; Zhang, P.-H.; Zhou, Q. Food-Drug Interactions Precipitated by Fruit Juices Other than Grapefruit Juice: An Update Review. *J. Food Drug Anal.* **2018**, *26*, S61–S71. [[CrossRef](#)]
24. Han, M.; Xu, J.; Lin, Y. Approaches of Formulation Bridging in Support of Orally Administered Drug Product Development. *Int. J. Pharm.* **2022**, *629*, 122380. [[CrossRef](#)] [[PubMed](#)]
25. Yee, S.W.; Vora, B.; Oskotsky, T.; Zou, L.; Jakobsen, S.; Enogieru, O.J.; Koleske, M.L.; Kosti, I.; Rödin, M.; Sirota, M.; et al. Drugs in COVID-19 Clinical Trials: Predicting Transporter-Mediated Drug-Drug Interactions Using in Vitro Assays and Real-World Data. *Clin. Pharmacol. Ther.* **2021**, *110*, 108–122. [[CrossRef](#)] [[PubMed](#)]
26. Karlgren, M.; Simoff, I.; Backlund, M.; Wegler, C.; Keiser, M.; Handin, N.; Müller, J.; Lundquist, P.; Jareborg, A.C.; Oswald, S.; et al. A CRISPR-Cas9 Generated MDCK Cell Line Expressing Human MDR1 without Endogenous Canine MDR1 (CABC1): An Improved Tool for Drug Efflux Studies. *J. Pharm. Sci.* **2017**, *106*, 2909–2913. [[CrossRef](#)] [[PubMed](#)]
27. Simoff, I.; Karlgren, M.; Backlund, M.; Lindström, A.C.; Gaugaz, F.Z.; Matsson, P.; Artursson, P. Complete Knockout of Endogenous Mdr1 (Abcb1) in MDCK Cells by CRISPR-Cas9. *J. Pharm. Sci.* **2016**, *105*, 1017–1021. [[CrossRef](#)] [[PubMed](#)]
28. Wegler, C.; Gazit, M.; Issa, K.; Subramaniam, S.; Artursson, P.; Karlgren, M. Expanding the Efflux in Vitro Assay Toolbox: A CRISPR-Cas9 Edited MDCK Cell Line with Human BCRP and Completely Lacking Canine MDR1. *J. Pharm. Sci.* **2021**, *110*, 388–396. [[CrossRef](#)] [[PubMed](#)]
29. Khuri, N.; Zur, A.A.; Wittwer, M.B.; Lin, L.; Yee, S.W.; Sali, A.; Giacomini, K.M. Computational Discovery and Experimental Validation of Inhibitors of the Human Intestinal Transporter OATP2B1. *J. Chem. Inf. Model.* **2017**, *57*, 1402–1413. [[CrossRef](#)] [[PubMed](#)]
30. In Vitro Drug Interaction Studies—Cytochrome P450 Enzyme- and Transporter-Mediated Drug Interactions Guidance for Industry. Available online: <https://www.fda.gov/media/134582/download> (accessed on 20 December 2023).
31. Sudsakorn, S.; Bahadduri, P.; Fretland, J.; Lu, C. 2020 FDA Drug-Drug Interaction Guidance: A Comparison Analysis and Action Plan by Pharmaceutical Industrial Scientists. *Curr. Drug Metab.* **2020**, *21*, 403–426. [[CrossRef](#)] [[PubMed](#)]
32. Zhang, J.; Selaya, S.D.; Shakleya, D.; Mohammad, A.; Faustino, P.J. Rapid Quantitation of Four Nitrosamine Impurities in Angiotensin Receptor Blocker Drug Substances. *J. Pharm. Sci.* **2023**, *112*, 1246–1254. [[CrossRef](#)]
33. Yamashiro, W.; Maeda, K.; Hirouchi, M.; Adachi, Y.; Hu, Z.; Sugiyama, Y. Involvement of Transporters in the Hepatic Uptake and Biliary Excretion of Valsartan, a Selective Antagonist of the Angiotensin II AT1-Receptor, in Humans. *Drug Metab. Dispos.* **2006**, *34*, 1247–1254. [[CrossRef](#)]
34. Homšak, M.; Trampuž, M.; Naveršnik, K.; Kitanovski, Z.; Žnidarič, M.; Kiefer, M.; Časar, Z. Assessment of a Diverse Array of Nitrite Scavengers in Solution and Solid State: A Study of Inhibitory Effect on the Formation of Alkyl-Aryl and Dialkyl N-Nitrosamine Derivatives. *Processes* **2022**, *10*, 2428. [[CrossRef](#)]

35. Nabekura, T.; Yamaki, T.; Hiroi, T.; Ueno, K.; Kitagawa, S. Inhibition of Anticancer Drug Efflux Transporter P-Glycoprotein by Rosemary Phytochemicals. *Pharmacol. Res.* **2010**, *61*, 259–263. [[CrossRef](#)] [[PubMed](#)]
36. Lee, K.-R.; Chang, J.-E.; Yoon, J.; Jin, H.; Chae, Y.-J. Findings on in Vitro Transporter-Mediated Drug Interactions and Their Follow-up Actions for Labeling: Analysis of Drugs Approved by US FDA between 2017 and 2021. *Pharmaceutics* **2022**, *14*, 2078. [[CrossRef](#)] [[PubMed](#)]

Disclaimer/Publisher's Note: The statements, opinions and data contained in all publications are solely those of the individual author(s) and contributor(s) and not of MDPI and/or the editor(s). MDPI and/or the editor(s) disclaim responsibility for any injury to people or property resulting from any ideas, methods, instructions or products referred to in the content.